

ADP-19-6/T1086
LTH 1200
DESY 19-053

Isospin splittings in the decuplet baryon spectrum from dynamical QCD+QED

R. Horsley¹, Z. Koumi², Y. Nakamura³, H. Perlt⁴,
D. Pleiter^{5,6}, P.E.L. Rakow⁷, G. Schierholz⁸, A. Schiller⁴,
H. Stüben⁹, R.D. Young² and J.M. Zanotti²

¹ School of Physics and Astronomy, University of Edinburgh, Edinburgh EH9 3FD, UK

² CSSM, Department of Physics, University of Adelaide, SA, Australia

³ RIKEN Center for Computational Science, Kobe, Hyogo 650-0047, Japan

⁴ Institut für Theoretische Physik, Universität Leipzig, 04109 Leipzig, Germany

⁵ Jülich Supercomputer Centre, Forschungszentrum Jülich, 52425 Jülich, Germany

⁶ Institut für Theoretische Physik, Universität Regensburg, 93040 Regensburg, Germany

⁷ Theoretical Physics Division, Department of Mathematical Sciences, University of Liverpool, Liverpool L69 3BX, UK

⁸ Deutsches Elektronen-Synchrotron DESY, 22603 Hamburg, Germany

⁹ Regionales Rechenzentrum, Universität Hamburg, 20146 Hamburg, Germany

CSSM/QCDSF/UKQCD Collaboration

Abstract. We report a new analysis of the isospin splittings within the decuplet baryon spectrum. Our numerical results are based upon five ensembles of dynamical QCD+QED lattices. The analysis is carried out within a flavour-breaking expansion which encodes the effects of breaking the quark masses and electromagnetic charges away from an approximate SU(3) symmetric point. The results display total isospin splittings within the approximate SU(2) multiplets that are compatible with phenomenological estimates. Further, new insight is gained into these splittings by separating the contributions arising from strong and electromagnetic effects. We also present an update of earlier results on the octet baryon spectrum.

1. Introduction

Isospin symmetry is so prevalent in the description of hadronic systems that the significance of a potential violation of this symmetry is often taken for granted. In the context of spectroscopy, isospin symmetry is manifest in the approximate degeneracy of isospin multiplets. Using this approximate symmetry to inform the interpretation of states can be incredibly powerful. Nevertheless, violations of this symmetry will become significant at some degree of precision. Isospin splittings in the ground state hyperons are known to be as much as 8 MeV. Phenomenological estimates suggest splittings in the decuplet baryons to be of a similar size [1]. Given that modern analyses are able to achieve (real part of the) pole positions at a precision of ± 1 MeV precision for the Δ -baryons [2,3], there is an opportunity to revisit analyses of isospin violation in low-energy πN scattering [4,5].

Beyond spectroscopy, it is also worth noting that the determination of isospin violation is relevant to a range of physical phenomena, including the flavour decomposition of nucleon structure [6–9]; tests of neutrino-nucleus interactions [10,11]; precision constraints on CKM [12,13] matrix elements from leptonic [14,15] and semi-leptonic [16] decay rates; and quark mass parameters [17–20]. In addition, the interplay of the coupled gauge theories in the nonperturbative domain offers a unique theoretical playground to explore. These extended motivations have prompted intensive effort in recent years to introduce electromagnetic effects in numerical lattice QCD studies [21–31] — building upon the pioneering work of Duncan, Eichten & Thacker [32].

In the present work, we perform simulations in dynamically-coupled QCD+QED [27,28], where the electric charges of sea-quark loops are included in the fermion determinant. In this work, the hadron spectrum calculations are performed across $32^3 \times 64$ and $48^3 \times 96$ lattices with up to 3 distinct sea quark mass combinations. Partially-quenched correlators are employed to further constrain flavour symmetry breaking effects. Starting from an SU(3) symmetric point inspired by Dashen’s relation [33], we use a flavour symmetry breaking expansion [28] to extrapolate to the physical quark masses and interpolate to the physical QED coupling — where our underlying gauge ensembles use an unphysically-large $\alpha_{\text{QED}} \sim 0.1$ to enhance the signal strength in the electromagnetic effects. In addition to providing isospin splittings among the decuplet multiplets, we also present updated results for the octet baryons.

The manuscript proceeds as follows: Section II reviews the form of the flavour-symmetry breaking expansions, including a description of the “Dashen scheme” used to distinguish electromagnetic and quark mass effects; Section 3 provides the lattice simulation details; Section 4 presents the lattice spectra results, including the flavour-breaking fits and treatment of finite-size effects; results and discussion follow in Section 5; and we conclude in Section 6.

2. Mass expansions

The approximate SU(3) flavour symmetry of nature has provided tremendous insight into strong interaction phenomenology. In recent lattice studies of pure QCD, we have exploited this symmetry by formulating an SU(3) expansion about a point of exact flavour symmetry [34]. The key to these investigations has been to use a starting point where the degenerate light (up, down and strange) quark mass is approximately equal

to the average of the corresponding physical masses, $\bar{m} = (m_u + m_d + m_s)/3$. As a consequence, when quark masses are tuned to lie on a trajectory that holds \bar{m} fixed at its physical value, flavour-singlet quantities only vary at second order in the dominant SU(3) breaking parameter $\delta m_q = m_q - \bar{m}$. This particular value is chosen such that lattice determinations of flavour-singlet quantities, such as $X_\pi^2 = (2m_K^2 + m_\pi^2)/3$, take their physical value. The extrapolation to the physical point along a trajectory with $\bar{m} = \text{constant}$ is simplified by the reduced set of operators that contribute to the quark mass variation [34]. Isospin violating effects arising from the quark mass difference $m_d - m_u$ are also naturally incorporated into the formulation [35].

Upon inclusion of electromagnetic effects, we wish to further exploit the perturbative breaking of SU(3) symmetry. The electromagnetic renormalisation of the quark masses makes it impossible to rigorously define equality of the light quark masses $m_u = m_d$ in a scheme-invariant fashion. Nevertheless, by choosing an appropriate renormalisation condition, we can ensure that electromagnetic effects can be treated perturbatively. Inspired by the Dashen relation [33], we impose the condition that the QCD component of neutral pseudoscalar mesons at the symmetric point can be parameterised identically and hence are equal. In practice, our tuning procedure requires that the bare quark masses, m_q (or κ_q in the case of Wilson fermions), at the SU(3) symmetric point are chosen such that all neutral (connected) pseudoscalar mesons $M(q\bar{q})$ are equal, i.e. $M^2(u\bar{u}) \approx M^2(d\bar{d}) = M^2(s\bar{s})$, where equality between $M^2(d\bar{d})$ and $M^2(s\bar{s})$ at the symmetric point is exact due to the fact that d and s quarks have the same charge. Further details of the Dashen scheme and the associated tuning can be found in Ref. [28].

Following the procedure outlined in Ref. [34], adapted to incorporate electromagnetic corrections [28], we obtain the relevant flavour-breaking expressions for our hadron masses. The flavour-breaking expansion of the pseudoscalar masses to NLO was reported in Ref. [28], however we quote the result here for completeness, albeit with a slight rearrangement of the terms

$$\begin{aligned}
M^2(a\bar{b}) = & M_0^2 + \alpha(\delta\mu_a + \delta\mu_b) + \beta_1(\delta\mu_a^2 + \delta\mu_b^2) \\
& + \beta_2(\delta\mu_a - \delta\mu_b)^2 + \beta_1^{EM}(e_a^2 + e_b^2) + \beta_2^{EM}(e_a - e_b)^2 \\
& + \gamma_1^{EM}(e_a^2\delta\mu_a + e_b^2\delta\mu_b) + \gamma_2^{EM}(e_a e_b)(\delta\mu_a + \delta\mu_b) \\
& + \gamma_3^{EM}(e_b^2\delta\mu_a + e_a^2\delta\mu_b) \\
& + c_1(\delta m_u + \delta m_d + \delta m_s) \\
& + c_2[\delta m_u^2 + \delta m_d^2 + \delta m_s^2 - (\delta m_u \delta m_d + \delta m_u \delta m_s + \delta m_d \delta m_s)] \\
& + c_3(\delta m_u + \delta m_d + \delta m_s)^2 + c_4(e_u^2 \delta m_u + e_d^2 \delta m_d + e_s^2 \delta m_s) \\
& + c_1^{EM}(e_u^2 + e_d^2 + e_s^2) + c_2^{EM}(e_u e_d + e_u e_s + e_d e_s) \\
& + c_3^{EM}(e_u^2 + e_d^2 + e_s^2)(\delta\mu_a + \delta\mu_b). \tag{1}
\end{aligned}$$

In this expansion, the valence quark charges are indicated by $e_{a,b}$ and the sea quark charges by $e_{u,d,s}$. The valence and sea quark mass deviations from the SU(3) symmetric point are respectively denoted by

$$\delta\mu_{a,b} = \mu_{a,b} - \bar{m}, \quad \delta m_{u,d,s} = m_{u,d,s} - \bar{m}. \tag{2}$$

These quark mass variations are evaluated in the Dashen scheme [28], where the distance from the symmetric point to the chiral limit, m_q^{sym} , is defined to be

independent of the quark charge, hence absorbing the quark electromagnetic self energy into the quark mass parameter.

Given that our framework is to approach the physical point along a trajectory that holds the singlet quark mass approximately constant[‡], we can neglect the c_1 and c_3 terms. Furthermore, the span of our sea quark masses are unable to provide any meaningful constraint on terms involving the sea masses. In particular, we neglect c_2 as $\mathcal{O}(\delta m^2)$ and c_4 as $\mathcal{O}(\alpha \delta m)$. The c^{EM} terms could be determined with simulations at different values of the QED gauge coupling, however in our present study these terms are simply absorbed into a redefinition of the relevant expansion parameters to give

$$\begin{aligned}
M^2(a\bar{b}) = & M_0^2 + \alpha(\delta\mu_a + \delta\mu_b) + \beta_1(\delta\mu_a^2 + \delta\mu_b^2) \\
& + \beta_2(\delta\mu_a - \delta\mu_b)^2 + \beta_1^{EM}(e_a^2 + e_b^2) + \beta_2^{EM}(e_a - e_b)^2 \\
& + \gamma_1^{EM}(e_a^2\delta\mu_a + e_b^2\delta\mu_b) + \gamma_2^{EM}(e_a e_b)(\delta\mu_a + \delta\mu_b) \\
& + \gamma_3^{EM}(e_b^2\delta\mu_a + e_a^2\delta\mu_b). \tag{3}
\end{aligned}$$

To the same order in the flavour-breaking parameters, we write the general expressions for the octet baryons:

$$\begin{aligned}
M(aab) = & M_0 + \alpha_1(2\delta\mu_a + \delta\mu_b) + \alpha_2\delta\mu_a \\
& + \beta_1(2\delta\mu_a^2 + \delta\mu_b^2) + \beta_2(\delta\mu_a^2 + 2\delta\mu_a\delta\mu_b) + \beta_3(\delta\mu_a^2) \\
& + \beta_1^{EM}(2e_a^2 + e_b^2) + \beta_2^{EM}(e_a^2 + 2e_a e_b) + \beta_3^{EM}(e_a^2) \\
& + \gamma_1^{EM}(2e_a^2\delta\mu_a + e_b^2\delta\mu_b) + \gamma_2^{EM}[2\delta\mu_a e_a(e_a + e_b) + 2\delta\mu_b e_b e_a] \\
& + \gamma_3^{EM}(2\delta\mu_a e_a e_b + \delta\mu_b e_a^2) + \gamma_4^{EM}(2\delta\mu_a(e_a^2 + e_b^2) + 2\delta\mu_b e_a^2) \\
& + \gamma_5^{EM}\delta\mu_a e_a^2 + \gamma_6^{EM}\delta\mu_a e_a e_b, \tag{4}
\end{aligned}$$

and the decuplet baryons:

$$\begin{aligned}
M(abc) = & M_0 + \alpha_1(\delta\mu_a + \delta\mu_b + \delta\mu_c) \\
& + \beta_1(\delta\mu_a^2 + \delta\mu_b^2 + \delta\mu_c^2) + \beta_2(\delta\mu_a\delta\mu_b + \delta\mu_a\delta\mu_c + \delta\mu_b\delta\mu_c) \\
& + \beta_1^{EM}(e_a^2 + e_b^2 + e_c^2) + \beta_2^{EM}(e_a e_b + e_a e_c + e_b e_c) \\
& + \gamma_1^{EM}(e_a^2\delta\mu_a + e_b^2\delta\mu_b + e_c^2\delta\mu_c) \\
& + \gamma_2^{EM}[\delta\mu_a e_a(e_b + e_c) + \delta\mu_b e_b(e_a + e_c) + \delta\mu_c e_c(e_a + e_b)] \\
& + \gamma_3^{EM}(\delta\mu_a e_b e_c + \delta\mu_b e_a e_c + \delta\mu_c e_a e_b) \\
& + \gamma_4^{EM}[\delta\mu_a(e_b^2 + e_c^2) + \delta\mu_b(e_a^2 + e_c^2) + \delta\mu_c(e_a^2 + e_b^2)]. \tag{5}
\end{aligned}$$

As argued above, we have already dropped the terms involving the sea quark masses and charges. We note that for any $f(M)$ an SU(3) flavour and charge breaking expansion can be made. For heavy quark masses, due to curvature in the numerical data, it was found [36] to be advantageous to expand M^2 ; here as the quark mass range used is smaller it is sufficient to consider an expansion of M .

[‡] Note that in pure QCD the singlet quark mass can be held constant exactly, but once electromagnetism is included, this is only approximately true due to the different quark charges.

Table 1. Summary of lattice ensemble details.

β	e^2	V	$\kappa_u, +2/3$	$\kappa_d, -1/3$	$\kappa_s, -1/3$	Ensemble
5.50	1.25	$32^3 \times 64$	0.124362	0.121713	0.121713	1
5.50	1.25	$32^3 \times 64$	0.124440	0.121676	0.121676	2
5.50	1.25	$32^3 \times 64$	0.124508	0.121821	0.121466	3
5.50	1.25	$48^3 \times 96$	0.124362	0.121713	0.121713	4
5.50	1.25	$48^3 \times 96$	0.124440	0.121676	0.121676	5

3. Lattice matters

The QCD+QED action we are using in this study is given by

$$S = S_G + S_A + S_F^u + S_F^d + S_F^s \quad (6)$$

where S_G is the tree-level Symanzik improved SU(3) gauge action; S_A is the noncompact U(1) gauge action of the photon; and S_F^q is the fermion action for each quark flavour, q . The photon action is,

$$S_A = \frac{1}{2e^2} \sum_{x, \mu < \nu} (A_\mu(x) + A_\nu(x + \mu) - A_\mu(x + \nu) - A_\nu(x))^2. \quad (7)$$

For the fermion action we employ the nonperturbatively $\mathcal{O}(a)$ -improved SLiNC action [37]

$$S_F^q = \sum_x \left\{ \frac{1}{2} \sum_\mu \left[\bar{q}(x)(\gamma_\mu - 1)e^{-ie_q A_\mu(x)} \tilde{U}_\mu(x) q(x + \hat{\mu}) - \bar{q}(x)(\gamma_\mu + 1)e^{ie_q A_\mu(x)} \tilde{U}_\mu^\dagger(x - \hat{\mu}) q(x - \hat{\mu}) \right] + \frac{1}{2\kappa_q} \bar{q}(x) q(x) - \frac{1}{4} c_{SW} \sum_{\mu\nu} \bar{q}(x) \sigma_{\mu\nu} F_{\mu\nu} q(x) \right\} \quad (8)$$

where \tilde{U}_μ is a single-iterated mild stout-smear link. The clover coefficient c_{SW} has been computed non-perturbatively for pure QCD [37] and we do not include the QED clover term.

Simulations are carried out on lattice volumes of size $32^3 \times 64$ and $48^3 \times 96$. The sea quark κ values are shown in Table 1, using charges of $e_u = +2/3$, $e_d = e_s = -1/3$. The strong coupling was chosen to be $\beta = 5.50$ and the electromagnetic coupling was chosen to be $e^2 = 1.25$, about ten times greater than physical. These choices lead to a lattice spacing of $a = 0.068(1)\text{fm}$ [28]. Further details can be found in Refs. [27, 28]. In order to better constrain the *a priori* unknown coefficients in the flavour-breaking expansions, we employ up to eight different partially-quenched valence quarks corresponding to neutral pseudoscalar meson masses in the range $225 \text{ MeV} \lesssim M(q\bar{q}) \lesssim 765 \text{ MeV}$ and valence quark charges $e_{a,b} = 0, -1/3, +2/3$. Hadron correlators are evaluated in the so-called QED_L formulation [38], where the zero mode of the photon field is eliminated on each time slice before computing the valence quark propagators.

Hadron masses are computed from two-point correlation functions using conventional techniques. In particular, for baryons we construct zero-momentum two-point functions as

$$C(t) = \sum_{\vec{x}} \text{Tr} \Gamma \langle \chi(\vec{x}, t) \bar{\chi}(0) \rangle, \quad (9)$$

for some choice of baryon spin projection matrix, Γ , e.g. for spin averaged, $\Gamma = (1 + \gamma_4)/2$. For octet baryons, we employ the interpolating operator in terms of a doubly-represented quark of flavour, q_1 , and a singly-represented quark of flavour, q_2

$$\chi(\vec{x}, t) = \epsilon^{abc} (q_1^{aT}(\vec{x}, t) C \gamma_5 q_2^b(\vec{x}, t)) q_1^c(\vec{x}, t), \quad (10)$$

where here a, b, c are colour labels. In the following, given the partially quenched nature of our simulations, we distinguish flavour by the electric charge carried by a quark rather than its mass. For example, when the combination uud occurs in the following discussion, this refers to an octet baryon where its doubly-represented quark has charge $+2/3$ while the singly-represented quark has charge $-1/3$. For decuplet baryons we choose an explicit spin-projection for the scalar diquark of the interpolating operator that contains doubly- and singly-represented quarks

$$\chi(\vec{x}, t) = \frac{1}{\sqrt{3}} \epsilon^{abc} \left[2 (q_1^{aT}(\vec{x}, t) C \gamma_- q_2^b(\vec{x}, t)) q_1^c(\vec{x}, t) + (q_1^{aT}(\vec{x}, t) C \gamma_- q_1^b(\vec{x}, t)) q_2^c(\vec{x}, t) \right], \quad (11)$$

where $\gamma_- = (\gamma_2 + i\gamma_1)/2$. We note that correlation functions for the Σ^{*0} , involving all three flavours of quarks, have not been computed in the present study.

In Figs. 1 and 2 we show examples of our results for the octet and decuplet baryon masses, respectively. These figures collect the partially-quenched results on both $48^3 \times 64$ ensembles listed in Table 1, plotted as function of the leading SU(3) breaking term $(2\delta\mu_a + \mu_b)$ from Eq. (4). The circles and triangles denote results from the $48^3 \times 96$ ensembles 4 and 5, respectively, as labelled in Table 1. To facilitate simpler comparisons with the fitted SU(3) expansion, the contributions from all other quark mass-dependent terms beyond $(2\delta\mu_a + \mu_b)$ in Eq. (4) have been subtracted from each mass point. As such the curves displayed are given by:

$$M^{(sub)}(aab) = M_0 + \alpha_1(2\delta\mu_a + \delta\mu_b) + \sum \beta_i^{EM} F_i(e_a, e_b), \quad (12)$$

where the functions F_i encode the appropriate quark-charge dependence as given by Eqs. 4 and 5. The residual scatter of the points around the line provides an indication of the quality of the global fit across the baryons. The slight difference in between the lines of the different panels provides a measure of the QED splittings encoded by the β^{EM} terms.

The left vertical dashed lines in Figs. 1 and 2 display the positions of the physical point for the corresponding baryons. For the octet baryons at charge $Q = 0$, the fit lines “interpolate” to the Ξ^+ and a mild extrapolation to the neutron point. Similarly, we see the Σ^+ and proton in the charge $Q = 1$ panel. For the decuplet we have chosen to display the corresponding $Q = -1$ and $Q = +1$ contours.

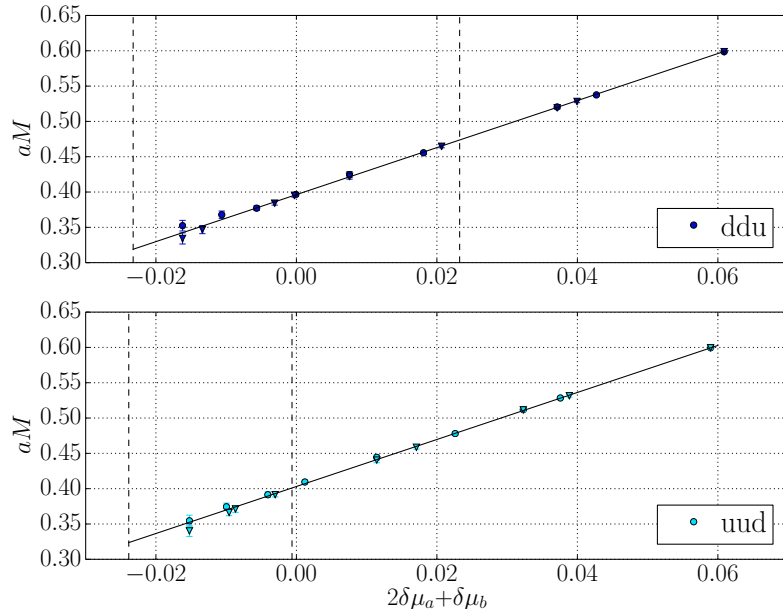


Figure 1. The dependence of the neutral, $Q = 0$, (top) and positively-charged, $Q = +1$, (bottom) octet baryons on the leading $SU(3)$ breaking term $(2\delta\mu_a + \mu_b)$ from Eq. (4), as described in the text. The circles and triangles denote results from the $48^3 \times 96$ ensembles 4 and 5, respectively, as labelled in Table 1. The vertical dashed lines indicate the locations of the baryon masses at the physical quark masses, as given in Table 2.

4. Analysis

4.1. Finite volume

In the present work, we just consider the leading finite-volume corrections associated with the electromagnetic interactions. Strong interaction effects are expected to be subdominant as they are exponentially suppressed by $\exp(-m_\pi L)$ whereas electromagnetic finite volume (FV) corrections are only power law suppressed, i.e. $1/L^n$. These infinite volume hadron masses are estimated in the effective field theory, NRQED_L, including corrections up to (and including) $\mathcal{O}(1/L^2)$ [25, 39, 40].[§]

Our full dataset includes results obtained from a subset of simulations which have all simulation parameters fixed except the physical volume. This allows us to assess the effects of the finite volume on our simulations as compared to the analytic expectations of Refs. [25, 39, 40]. By considering mass differences between isospin partners, strong finite-volume effects should cancel, leaving us with quantities that are primarily sensitive to electromagnetic finite-volume effects. We find that the splittings on our two volumes ($\sim 2.2, 3.3$ fm) are generally compatible with each other after accounting for the leading QED FV effects. When quoting our final values in the following sections, the results obtained from the finite-volume corrected $48^3 \times 96$ lattice

[§] We note that with our larger value of the electromagnetic coupling, $\alpha_{\text{QED}} \sim 0.1$, this expansion parameter is numerically comparable to the values of $1/(mL)$ in the NRQED expansion [41]. Nevertheless, Matzelle and Tiburzi [41] have shown that potentially-relevant higher-order terms in α_{QED} do not affect the expansion to $\mathcal{O}(1/L^2)$.

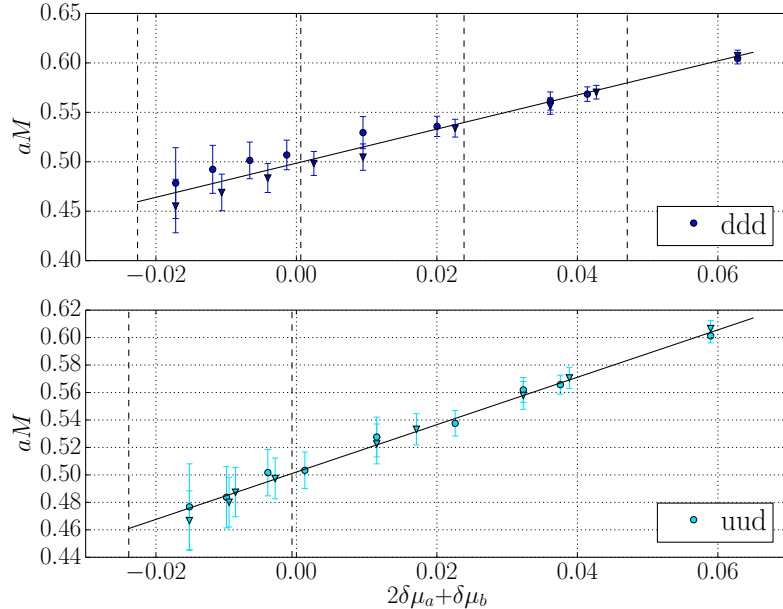


Figure 2. The dependence of the negative-charge, $Q = -1$, (top) and positively-charged, $Q = +1$, (bottom) decuplet baryons on the leading SU(3) breaking term ($2\delta\mu_a + \mu_b$) from Eq. (5), as described in the text. The circles and triangles denote results from the $48^3 \times 96$ ensembles 4 and 5, respectively, as labelled in Table 1. The vertical dashed lines indicate the locations of the baryon masses at the physical quark masses, as given in Table 2.

data provide the central values and statistical uncertainties. The difference between the two volumes, after correcting for the leading-order EM finite-volume effects and extrapolating to the physical point, provides a conservative estimate for the dominant systematic uncertainty.

4.2. The physical point

The first stage of our analysis is to identify the location of the quark mass parameters corresponding to the physical point. For this, we restrict ourselves to the meson sector following the procedure outlined in Ref. [28]. The general expansion of Eq. (3) is modified such that the QED contributions to the neutral pseudoscalar mesons are absorbed into the quark self-energy. This modification defines the Dashen quark mass parameters, δm_q^D , $\delta\mu_a^D$, which are then used to parameterise the deviation from the SU(3) origin. As described in Section 2, terms involving the c and c^{EM} coefficients have been neglected in this analysis. Upon fitting the resulting expression to the remainder of the pseudoscalar meson mass spectrum, the enhanced value of $\alpha_{\text{QED}} = 1.25/4\pi$ employed in our simulations is corrected by a linear rescaling of the fitted β^{EM} and γ^{EM} coefficients by a factor of $4\pi/(1.25 \times 137)$. Constraining the fits to three pieces of physical input, namely the physical π^0 , K^0 and K^+ masses, then leads to a determination of the lattice spacing and the bare quark masses at the physical point. These results are given in Table 2 for the larger $48^3 \times 96$ volume. We note that only three physical inputs are required to determine the four unknown parameters, as we

have the additional constraint built into our simulations that the average quark mass, $\bar{m} = (m_u + m_d + m_s)/3$, is held fixed, i.e. $\delta m_u + \delta m_d + \delta m_s = 0$. Using the parameters given in Table 2, we are able to provide a prediction for the π^+ mass, which is provided in Table 3 in the form of a mass splitting from the π^0 . The result from the present work is in agreement with that from [28], however we note the improved statistical precision of the current work due to the inclusion of the additional ensembles away from the SU(3) symmetric point summarised in Table 1.

Table 2. Dashen quark mass parameters at the physical point and the inverse lattice spacing.

$a\delta m_u^D$	$a\delta m_d^D$	$a\delta m_s^D$	a^{-1}/GeV
-0.00786 (1)	-0.00728 (2)	0.0151 (2)	2.906 (12)

4.3. Baryons

At this stage we have completely described our Dashen scheme and have predictions for the physical quark masses and the lattice spacing for each volume. Hence we are now in a position to fit the finite-volume corrected, partially quenched octet and decuplet baryon masses to the flavour-breaking expansions given in Eqs. (4) and (5) with the bare quark masses, $\delta\mu_q$ replaced by the Dashen mass $\delta\mu_q^D$.

Previous work has shown that the light hadron spectrum in pure QCD is well described along our $\bar{m} = \text{constant}$ trajectory by flavour breaking expansions that are linear in the flavour breaking quark mass parameter over the entire mass range from the SU(3)-symmetric point to the physical point, with only small corrections provided by terms quadratic in the flavour-breaking parameter [34]. A summary of the fit parameters for the $48^3 \times 96$ lattice ensembles is presented in Appendix A.

We note that the reduced χ^2 values indicate that the fits are suitably able to describe the data. To visualise the multi-dimensional fit, we show the central values of the fit parameterisation against the (finite-volume corrected) lattice spectra in Figs. 1 and 2.

5. Results & Discussion

5.1. Octet baryons

Using the preferred fits we can extrapolate our spectrum to the physical point, as determined within the meson sector. The absolute masses of the baryon octet are summarised in Table 4, where we see excellent agreement with the experimental values for the proton and neutron masses, while we observe multiple- σ discrepancies as the number of strange quarks in the baryons is increased. This is perhaps an indication of a slight mismatch in our tuning of the singlet quark mass. This effect, however, will not affect the results for isospin splittings presented in the remainder of this paper.

Given the high degree of correlation in the mass determinations, the isospin splittings are determined to much better precision and are displayed in Figure 3 for our two lattice volumes.

These mass splittings are summarised in Table 3 and serve as an update to our earlier work [27] which was based on only a single set of sea quark masses, namely

Table 3. Predicted mass splittings for π^+ and octet baryons in the Dashen scheme, including a separation into QCD and QED contributions in the Dashen scheme. π^0 assumed to be the state $(u\bar{u} - d\bar{d})/\sqrt{2}$. Experimental mass splittings [3] are also given for comparison. All values quoted in MeV.

	$\pi^+ - \pi^0$	$n - p$	$\Sigma^- - \Sigma^+$	$\Xi^- - \Xi^0$
QED	5.86(14)(40)	-1.53(25)(50)	-0.29(24)(10)	1.19(15)(20)
QCD	—	2.79(67)(40)	8.58(72)(70)	5.79(28)(80)
Total	—	1.27(75)(50)	8.29(77)(25)	6.95(25)(90)
Experiment	4.59	1.30	8.08	6.85

Table 4. Extrapolated masses for the octet baryons in the Dashen scheme, showing comparison with the experimental masses [3]. Only the maximally-charged state of each isospin multiplet is shown. All values quoted in MeV.

	p	Σ^+	Ξ^0
	939(14)(56)	1165(11)(23)	1276(6)(19)
Experiment	938.3	1189.4	1314.8

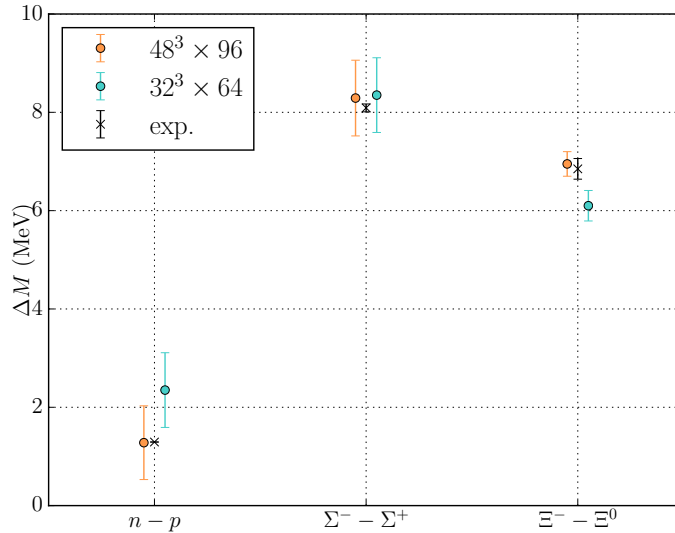


Figure 3. Octet mass splitting with the average octet family mass subtracted. This includes EM effects. The black crosses are experimental data. The coloured points are estimates generated from our lattice analysis.

ensembles 1 and 4 in Table 1. We note that in Ref. [27] the photon zero modes were treated dynamically, requiring an effective kinetic energy to be subtracted at the analysis stage. The first uncertainty shown in Table 1 is statistical, while the second provides an estimate of the finite-size systematic error as described in the previous section. We note that since our simulations are performed at only a single value of the lattice spacing, no continuum extrapolation is possible.

In Ref. [28] we provided a prescription for converting electromagnetic mass contributions between Dashen and $\overline{\text{MS}}$ schemes, however to leading order this has no effect on the central values and hence we only quote our Dashen scheme results. To separate QED and QCD, we note the γ^{EM} terms in Eqs. 4 and 5 describe a product of e^2 and $\delta\mu$ effects. We distinguish the isospin-breaking effects arising from these terms as either being: QED, when $\delta\mu_u = \delta\mu_d$; QCD, when $e_u = e_d$; or a remaining (and small) second-order isospin-breaking effect. For example, terms involving the product $(e_u - e_d)(\delta\mu_u + \delta\mu_d)$ is attributed to QED, whereas $(e_u + e_d)(\delta\mu_u - \delta\mu_d)$ is attributed to QCD. The former vanish if the up and down charges are equal, while the latter vanish if the masses are equal.

The electromagnetic splitting between the proton and neutron has seen considerable attention in recent years. Our result for the proton-neutron mass-splitting shows some preference to the dispersive analysis of Ref. [42], which finds -1.30 ± 0.47 MeV. In contrast, we see our result is slightly larger in magnitude than the values reported in Refs. [43] and [44, 45], though not in statistical disagreement. It is noted that the latter phenomenological studies display better agreement with the lattice results of the BMW Collaboration [25].

Figure 4 shows the breakdown between strong isospin breaking and electromagnetic effects for the octet baryons. The Ξ splittings are generally compatible with both phenomenological estimates [43] and the BMW lattice results [25]. We note that a direct comparison for the electromagnetic splitting in the Σ is not possible, since this is set to zero in the scheme prescribed in Ref. [25].

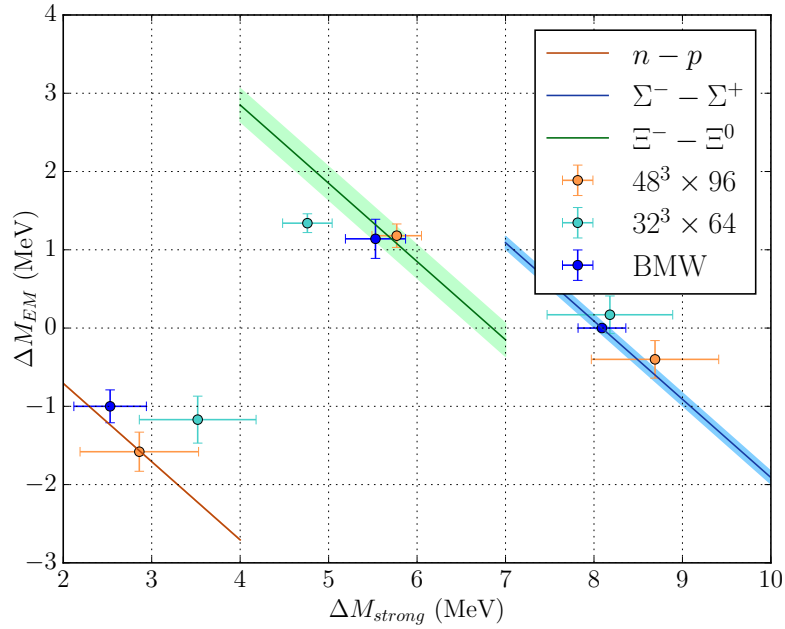


Figure 4. A decomposition of the octet splitting in terms of EM and strong isospin breaking effects. The BMW lattice points are from [25]. The lines represent a constraint placed by the experimental data.

5.2. Decuplet baryons

For the decuplet baryons, our analysis is restricted to the extrapolation of our lattice masses to the physical point based on the flavour-breaking expansion about the SU(3) symmetric point. That is, no attempt has been made in the present work to incorporate the effects of the resonant nature of the decuplet baryons at the physical quark masses — which necessarily lead to branch point singularities in the quark mass extrapolation [46, 47]. The isospin splittings within the decuplet baryons therefore represent a first estimate on the magnitude of these effects. A full treatment including mixing with multi-hadron states is left for future work.

As for the octet baryons, our decuplet expansion is fit to the electromagnetic finite-volume corrected lattice results. The absolute masses themselves do not compare so favourably with experimental determinations, as shown in Table 5. Within the

Table 5. Absolute masses for the maximally-charged state for each isospin multiplet within the decuplet. All values quoted in MeV.

	Δ^{++}	Σ^{*+}	Ξ^{*0}	Ω
This work	1304(59)(6)	1425(38)(8)	1542(26)(9)	1656(21)(8)
Experiment	1231	1383	1532	1672

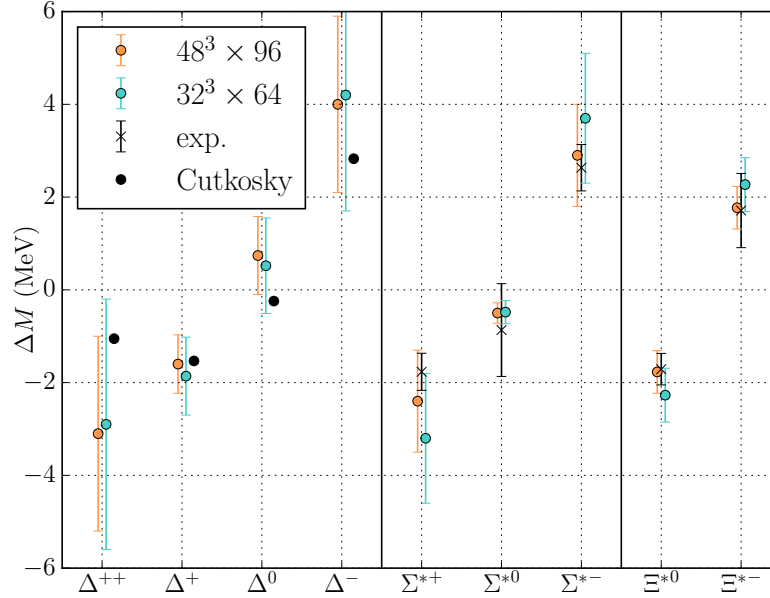
quoted uncertainties we observe that the absolute masses at the physical point are compatible with the experimental masses. Nevertheless, it is possible that there is a systematic uncertainty that is causing an underestimate of the overall scale of the SU(3) breaking between these states. This could be due to the fact that our simulations are performed at and around the SU(3) symmetric point where the Δ and Σ^* states are stable states. However, in the physical system the Δ and Σ^* states are unstable and decay, e.g. to $\Delta \rightarrow \pi + N$, where the net mass of the $\pi + N$ system is significantly lower than the three quark state. The opening of these decay channels is certainly anticipated to affect the extrapolation to the physical point [46]. This physics of the decays would become less prominent for Ξ^* and irrelevant for the Ω , which is stable under the strong interaction.

Assuming that the threshold effects do not have a strong influence on the isospin-violating parts, we expect that the magnitudes and orderings of the splittings to be indicative of the expected behaviour at the physical point. We highlight some various selected splittings of phenomenological interest in Table 6. The combination $\Delta^{++} + \Delta^- - \Delta^+ - \Delta^0$ is selected as it eliminates the leading strong isospin violation, and hence provides a purely electromagnetic effect. The difference $\Delta^0 - \Delta^{++}$ is reported by the PDG. The particular combination $\Delta^- - \Delta^{++} + \frac{1}{3}(\Delta^0 - \Delta^+)$ can be isolated experimentally by considering the difference between π^+ and π^- cross sections on deuteron targets, as reported in Ref. [48]. For the Σ^* baryons, again $\Sigma^{*+} + \Sigma^{*-} - 2\Sigma^{*0}$ removes the leading strong isospin breaking, leaving a purely electromagnetic effect. To mimic the analogous splitting of the octet baryons we display $\Sigma^{*-} - \Sigma^{*+}$, which is observed to be dominated by the quark mass differences. Similarly we find that $\Xi^{*-} - \Xi^{*0}$ is also dominated by the strong effect, which is perhaps counterintuitive since the electromagnetic effect in Ξ^{*-} is repulsive while it is attractive in Ξ^{*0} .

The final mass splittings due to isospin breaking effects, both strong and electromagnetic, at the physical quark masses for all decuplet baryon on both volumes are shown in Figure 5. The mass splittings within each isospin multiplet are displayed

Table 6. Mass splittings for decuplet baryons. All values quoted in MeV.

	$\Delta^{++} + \Delta^- - \Delta^+ - \Delta^0$	$\Delta^0 - \Delta^{++}$	$\Delta^- - \Delta^{++} + \frac{1}{3}(\Delta^0 - \Delta^+)$
QED	1.7(14)(10)	-2.5(20)(13)	-2.7(26)(20)
QCD	-0.006(11)(6)	6.3(24)(5)	10.5(40)(10)
Total	1.7 (14)(10)	3.8(31)(5)	7.8(46)(5)
Cutkosky [1]	2.84–3.55	0.81–1.53	4.31–4.92
Exp./Pheno.	—	2.86(30) [49]	4.6(2) [48]
	$\Sigma^{*+} + \Sigma^{*-} - 2\Sigma^{*0}$	$\Sigma^{*-} - \Sigma^{*+}$	$\Xi^{*-} - \Xi^{*0}$
QED	1.5(7)(1)	-0.8(11)(7)	0.61(51)(60)
QCD	-0.0032(56)(30)	6.1(22)(2)	2.92(98)(1)
Total	1.5(7)(1)	5.3(23)(10)	3.54(98)(8)
Cutkosky [1]	1.42	4.56	3.09
PDG [3]	2.6(21)	4.4(6)	3.2(6)


Figure 5. Mass splittings within the isospin multiplets of decuplet baryons with respect to the average multiplet mass (see Eq. (13)), including both strong and electromagnetic effects. The black crosses for Σ^* and Ξ^* baryons are experimental data [3], while the black circles for Δ baryons indicate a fit to experimental data [1].

as the difference of each mass from the average of its respective multiplet. For example, the splittings in Delta baryons are given by:

$$\Delta M_B = M_B - \frac{1}{4}(M_{\Delta^{++}} + M_{\Delta^+} + M_{\Delta^0} + M_{\Delta^-}). \quad (13)$$

For the Σ^* and Ξ^* baryons we are able to compare our mass splittings directly with those obtained from experiment, indicated by the black crosses, while for the Δ

baryons we are only able to compare to a fit to experimental data [1]. The results shown in Figure 5 clearly agree with the experimental determinations, indicating that while the overall magnitude of our decuplet baryon masses are overestimated, potentially due to the fact that we haven't considered the full resonance structure of the strongly unstable baryons, the mass splittings within each multiplet can be accurately described by our QCD+QED simulation.

6. Conclusion

We have presented lattice QCD+QED results for the light baryon mass spectrum including both strong and electromagnetic isospin breaking effects. Our simulations are based on partially-quenched simulations with 2 volumes and up to three choices for the sea quark masses at and around the SU(3) symmetric point. For the octet baryons, this work represents an update to our earlier findings [27] which were obtained from only a single choice of sea quarks. Another difference to our previous work is the use of the QED_L formulation [38] for the valence quarks. We find excellent agreement between our results for the mass splittings of the isospin partners, $n - p$, $\Sigma^- - \Sigma^+$, $\Xi^- - \Xi^0$ and those observed experimentally. Our procedure also allows for the decomposition of these isospin-dependent mass splittings into strong and electromagnetic contributions with the Dashen scheme.

Qualitatively the absolute values of the masses of our decuplet spectrum are too large, although we have not yet considered how the pole position of a resonance can be affected by the multi-hadron strong decay modes in a finite volume which may account for some of this discrepancy. A description of the resonance nature of the decuplet baryon mass spectrum has only recently started to be addressed in pure QCD lattice simulations [50,51]. A full formalism to resolve resonant features of hadron scattering in a finite box, including the long-range Coulomb interactions, is yet to be developed.

The principle focus of the present work is the determination of the isospin breaking effects in the decuplet baryon mass spectrum. The lattice estimates for the mass splittings within the different isospin multiplets of the decuplet baryons, however, are in excellent agreement with the experimentally observed splittings in the case of the Σ^* and Ξ^* baryons, or a phenomenological fit using experimental data [1] in the case of the Δ baryons.

Acknowledgments

The numerical configuration generation (using the BQCD lattice QCD program [52]) and data analysis (using the Chroma software library [53]) was carried out on the IBM BlueGene/Q and HP Tesseract using DIRAC 2 resources (EPCC, Edinburgh, UK), the IBM BlueGene/Q (NIC, Jülich, Germany) and the Cray XC40 at HLRN (The North-German Supercomputer Alliance), the NCI National Facility in Canberra, Australia (supported by the Australian Commonwealth Government) and Phoenix (University of Adelaide). HP was supported by DFG Grant No. PE 2792/2-1. PELR was supported in part by the STFC under contract ST/G00062X/1 and RDY and JMZ were supported by the Australian Research Council Grants FT120100821, FT100100005, DP140103067 and DP190100297. We thank all funding agencies.

Appendix A. Fit parameters

In Table A1, we report the fit parameters of the flavour-breaking expansions.

Table A1. Expansion parameters as determined for the $48^3 \times 96$ volume. The terms involving the electromagnetic couplings have been scaled to the physical point by the factor $\alpha_{QED}^{\text{phys}}/\alpha_{QED}^{\text{lat}}$.

	Meson	Octet	Decuplet
M_0	0.020504(66)	0.3944(24)	0.494(11)
α_1	1.1703(47)	3.32(11)	1.73(40)
α_2	—	-1.71(23)	—
β_1	-0.17(22)	-20.7(40)	1.0(135)
β_2	1.51(12)	-14.2(13)	-2.9(45)
β_3	—	38.0(11)	—
β_1^{EM}	0.0001975(47)	0.00083(17)	0.00064(53)
β_2^{EM}	-0.0005222(37)	0.001032(55)	0.00042(18)
β_3^{EM}	—	-0.00022(33)	—
γ_1^{EM}	0.00435(26)	-0.0041(44)	0.012(17)
γ_2^{EM}	-0.00899(13)	0.0014(11)	0.003(5)
γ_3^{EM}	0.00526(21)	-0.0063(54)	0.0092(61)
γ_4^{EM}	—	0.0014(27)	-0.00011(70)
γ_5^{EM}	—	0.008(11)	—
γ_6^{EM}	—	0.016(12)	—
χ^2	183.74	47.12	20.35
DOF	105	112	118
χ^2/DOF	1.75	0.42	0.172

- [1] R. E. Cutkosky, “Isospin splitting in the baryon octet and decuplet,” *Phys. Rev.*, vol. C47, pp. 367–371, 1993.
- [2] A. Svarc, M. Hadžimehmedović, R. Omerović, H. Osmanović, and J. Stahov, “Poles of Karlsruhe-Helsinki KH80 and KA84 solutions extracted by using the Laurent-Pietarinen method,” *Phys. Rev.*, vol. C89, no. 4, p. 045205, 2014.
- [3] C. Patrignani *et al.*, “Review of Particle Physics,” *Chin. Phys.*, vol. C40, no. 10, p. 100001, 2016.
- [4] W. R. Gibbs, L. Ai, and W. B. Kaufmann, “Isospin breaking in low-energy pion nucleon scattering,” *Phys. Rev. Lett.*, vol. 74, pp. 3740–3743, 1995.
- [5] E. Matsinos, “Isospin violation in the pi N system at low-energies,” *Phys. Rev.*, vol. C56, pp. 3014–3025, 1997.
- [6] G. A. Miller, A. K. Opper, and E. J. Stephenson, “Charge symmetry breaking and QCD,” *Ann. Rev. Nucl. Part. Sci.*, vol. 56, pp. 253–292, 2006.
- [7] J. T. Londergan, J. C. Peng, and A. W. Thomas, “Charge Symmetry at the Partonic Level,” *Rev. Mod. Phys.*, vol. 82, pp. 2009–2052, 2010.
- [8] M. Wagman and G. A. Miller, “Charge Symmetry Breaking and Parity Violating Electron-Proton Scattering,” *Phys. Rev.*, vol. C89, no. 6, p. 065206, 2014. [Erratum: *Phys. Rev. C*91,no.1,019903(2015)].
- [9] P. E. Shanahan, R. Horsley, Y. Nakamura, D. Pleiter, P. E. L. Rakow, G. Schierholz, H. Stüben, A. W. Thomas, R. D. Young, and J. M. Zanotti, “Charge symmetry violation in the electromagnetic form factors of the nucleon,” *Phys. Rev.*, vol. D91, no. 11, p. 113006, 2015.
- [10] G. P. Zeller *et al.*, “A Precise determination of electroweak parameters in neutrino nucleon scattering,” *Phys. Rev. Lett.*, vol. 88, p. 091802, 2002. [Erratum: *Phys. Rev. Lett.*90,239902(2003)].
- [11] W. Bentz, I. C. Cloet, J. T. Londergan, and A. W. Thomas, “Reassessment of the NuTeV determination of the weak mixing angle,” *Phys. Lett.*, vol. B693, pp. 462–466, 2010.
- [12] N. Cabibbo, “Unitary Symmetry and Leptonic Decays,” *Phys. Rev. Lett.*, vol. 10, pp. 531–533, 1963. [648(1963)].
- [13] M. Kobayashi and T. Maskawa, “CP Violation in the Renormalizable Theory of Weak Interaction,” *Prog. Theor. Phys.*, vol. 49, pp. 652–657, 1973.
- [14] V. Cirigliano and H. Neufeld, “A note on isospin violation in $\text{P}12(\gamma)$ decays,” *Phys. Lett.*, vol. B700, pp. 7–10, 2011.
- [15] W. Lucha, D. Melikhov, and S. Simula, “Isospin breaking in the decay constants of heavy mesons from QCD sum rules,” *Phys. Lett.*, vol. B765, pp. 365–370, 2017.
- [16] V. Cirigliano, H. Neufeld, and H. Pichl, “ $\text{K}(e3)$ decays and CKM unitarity,” *Eur. Phys. J.*, vol. C35, pp. 53–65, 2004.
- [17] J. Gasser and H. Leutwyler, “Quark Masses,” *Phys. Rept.*, vol. 87, pp. 77–169, 1982.
- [18] H. Leutwyler, “Bounds on the light quark masses,” *Phys. Lett.*, vol. B374, pp. 163–168, 1996.
- [19] J. Gasser, A. Rusetsky, and I. Scimemi, “Electromagnetic corrections in hadronic processes,” *Eur. Phys. J.*, vol. C32, pp. 97–114, 2003.
- [20] G. Colangelo, S. Lanz, H. Leutwyler, and E. Passemar, “ $\eta \rightarrow 3\pi$: Study of the Dalitz plot and extraction of the quark mass ratio Q ,” *Phys. Rev. Lett.*, vol. 118, no. 2, p. 022001, 2017.
- [21] T. Blum, R. Zhou, T. Doi, M. Hayakawa, T. Izubuchi, S. Uno, and N. Yamada, “Electromagnetic mass splittings of the low lying hadrons and quark masses from 2+1 flavor lattice QCD+QED,” *Phys. Rev.*, vol. D82, p. 094508, 2010.
- [22] S. Aoki *et al.*, “1+1+1 flavor QCD + QED simulation at the physical point,” *Phys. Rev.*, vol. D86, p. 034507, 2012.
- [23] G. M. de Divitiis, R. Frezzotti, V. Lubicz, G. Martinelli, R. Petronzio, G. C. Rossi, F. Sanfilippo, S. Simula, and N. Tantalo, “Leading isospin breaking effects on the lattice,” *Phys. Rev.*, vol. D87, no. 11, p. 114505, 2013.
- [24] S. Borsanyi *et al.*, “Isospin splittings in the light baryon octet from lattice QCD and QED,” *Phys. Rev. Lett.*, vol. 111, no. 25, p. 252001, 2013.
- [25] S. Borsanyi *et al.*, “Ab initio calculation of the neutron-proton mass difference,” *Science*, vol. 347, pp. 1452–1455, 2015.
- [26] M. G. Endres, A. Shindler, B. C. Tiburzi, and A. Walker-Loud, “Massive photons: an infrared regularization scheme for lattice QCD+QED,” *Phys. Rev. Lett.*, vol. 117, no. 7, p. 072002, 2016.
- [27] R. Horsley *et al.*, “Isospin splittings of meson and baryon masses from three-flavor lattice QCD + QED,” *J. Phys.*, vol. G43, no. 10, p. 10LT02, 2016.
- [28] R. Horsley *et al.*, “QED effects in the pseudoscalar meson sector,” *JHEP*, vol. 04, p. 093, 2016.
- [29] D. Giusti, V. Lubicz, C. Tarantino, G. Martinelli, S. Sanfilippo, S. Simula, and N. Tantalo,

- “Leading isospin-breaking corrections to pion, kaon and charmed-meson masses with Twisted-Mass fermions,” *Phys. Rev.*, vol. D95, no. 11, p. 114504, 2017.
- [30] P. Boyle, V. Gülpers, J. Harrison, A. Jüttner, C. Lehner, A. Portelli, and C. T. Sachrajda, “Isospin breaking corrections to meson masses and the hadronic vacuum polarization: a comparative study,” *JHEP*, vol. 09, p. 153, 2017.
- [31] D. Giusti, V. Lubicz, G. Martinelli, C. T. Sachrajda, F. Sanfilippo, S. Simula, N. Tantalo, and C. Tarantino, “First lattice calculation of the QED corrections to leptonic decay rates,” *Phys. Rev. Lett.*, vol. 120, no. 7, p. 072001, 2018.
- [32] A. Duncan, E. Eichten, and H. Thacker, “Electromagnetic splittings and light quark masses in lattice QCD,” *Phys. Rev. Lett.*, vol. 76, pp. 3894–3897, 1996.
- [33] R. F. Dashen, “Chiral $SU(3) \times SU(3)$ as a symmetry of the strong interactions,” *Phys. Rev.*, vol. 183, pp. 1245–1260, 1969.
- [34] W. Bietenholz *et al.*, “Flavour blindness and patterns of flavour symmetry breaking in lattice simulations of up, down and strange quarks,” *Phys. Rev.*, vol. D84, p. 054509, 2011.
- [35] R. Horsley, J. Najjar, Y. Nakamura, D. Pleiter, P. E. L. Rakow, G. Schierholz, and J. M. Zanotti, “Isospin breaking in octet baryon mass splittings,” *Phys. Rev.*, vol. D86, p. 114511, 2012.
- [36] R. Horsley, J. Najjar, Y. Nakamura, H. Perlt, D. Pleiter, P. E. L. Rakow, G. Schierholz, A. Schiller, H. Stüben, and J. M. Zanotti, “Lattice determination of Sigma-Lambda mixing,” *Phys. Rev.*, vol. D91, no. 7, p. 074512, 2015.
- [37] N. Cundy *et al.*, “Non-perturbative improvement of stout-smearred three flavour clover fermions,” *Phys. Rev.*, vol. D79, p. 094507, 2009.
- [38] M. Hayakawa and S. Uno, “QED in finite volume and finite size scaling effect on electromagnetic properties of hadrons,” *Prog. Theor. Phys.*, vol. 120, pp. 413–441, 2008.
- [39] Z. Davoudi and M. J. Savage, “Finite-Volume Electromagnetic Corrections to the Masses of Mesons, Baryons and Nuclei,” *Phys. Rev.*, vol. D90, no. 5, p. 054503, 2014.
- [40] J.-W. Lee and B. C. Tiburzi, “Finite Volume Corrections to the Electromagnetic Mass of Composite Particles,” *Phys. Rev.*, vol. D93, no. 3, p. 034012, 2016.
- [41] M. E. Matzelle and B. C. Tiburzi, “Finite-Volume Corrections to Electromagnetic Masses for Larger-Than-Physical Electric Charges,” *Phys. Rev.*, vol. D95, no. 9, p. 094510, 2017.
- [42] A. Walker-Loud, C. E. Carlson, and G. A. Miller, “The Electromagnetic Self-Energy Contribution to $M_p - M_n$ and the Isovector Nucleon Magnetic Polarizability,” *Phys. Rev. Lett.*, vol. 108, p. 232301, 2012.
- [43] F. B. Erben, P. E. Shanahan, A. W. Thomas, and R. D. Young, “Dispersive estimate of the electromagnetic charge symmetry violation in the octet baryon masses,” *Phys. Rev.*, vol. C90, no. 6, p. 065205, 2014.
- [44] J. Gasser, M. Hoferichter, H. Leutwyler, and A. Rusetsky, “Cottingham formula and nucleon polarisabilities,” *Eur. Phys. J.*, vol. C75, no. 8, p. 375, 2015.
- [45] J. Gasser and H. Leutwyler, “Implications of Scaling for the Proton - Neutron Mass - Difference,” *Nucl. Phys.*, vol. B94, pp. 269–310, 1975.
- [46] R. D. Young, D. B. Leinweber, A. W. Thomas, and S. V. Wright, “Chiral analysis of quenched baryon masses,” *Phys. Rev.*, vol. D66, p. 094507, 2002.
- [47] V. Pascalutsa and M. Vanderhaeghen, “The Nucleon and delta-resonance masses in relativistic chiral effective-field theory,” *Phys. Lett.*, vol. B636, pp. 31–39, 2006.
- [48] E. Pedroni *et al.*, “A Study of Charge Independence and Symmetry from π^+ and π^- Total Cross-Sections on Hydrogen and Deuterium Near the 3,3 Resonance,” *Nucl. Phys.*, vol. A300, pp. 321–347, 1978.
- [49] A. B. Gridnev, I. Horn, W. J. Briscoe, and I. I. Strakovsky, “The K-matrix approach to the Delta - resonance mass splitting and isospin violation in low-energy π -N scattering,” *Phys. Atom. Nucl.*, vol. 69, pp. 1542–1551, 2006.
- [50] C. Alexandrou, J. W. Negele, M. Petschlies, A. V. Pochinsky, and S. N. Syritsyn, “Study of decuplet baryon resonances from lattice QCD,” *Phys. Rev.*, vol. D93, no. 11, p. 114515, 2016.
- [51] C. W. Andersen, J. Bulava, B. Hörz, and C. Morningstar, “Elastic $I = 3/2$ -wave nucleon-pion scattering amplitude and the $\Delta(1232)$ resonance from $N_f=2+1$ lattice QCD,” *Phys. Rev.*, vol. D97, no. 1, p. 014506, 2018.
- [52] T. Haar, Y. Nakamura, and H. Stüben, “An update on the BQCD Hybrid Monte Carlo program,” *EPJ Web Conf.*, vol. 175, p. 14011, 2018.
- [53] R. Edwards and B. Joo, “The Chroma software system for lattice QCD,” *Nucl. Phys. Proc. Suppl.*, vol. 140, p. 832, 2005. [[832\(2004\)](#)].